

Interval-Based AUC(iAUC): Extending ROC Analysis to Uncertainty-Aware Classification

Yuqi Li¹ Matthew M. Engelhard¹

¹Department of Biostatistics & Bioinformatics, Duke University
`{yuqi.li, m.engelhard}@duke.edu`

Abstract

In high-stakes risk prediction, quantifying uncertainty through interval-valued predictions is essential for reliable decision-making. However, standard evaluation tools like the receiver operating characteristic (ROC) curve and the area under the curve (AUC) are designed for point scores and fail to capture the impact of predictive uncertainty on ranking performance. We propose an uncertainty-aware ROC framework specifically for interval-valued predictions, introducing two new measures: AUC_L and AUC_U . This framework enables an informative three-region decomposition of the ROC plane, partitioning pairwise rankings into correct, incorrect, and uncertain orderings. This approach naturally supports selective prediction by allowing models to abstain from ranking cases with overlapping intervals, thereby optimizing the trade-off between abstention rate and discriminative reliability. We prove that under valid class-conditional coverage, AUC_L and AUC_U provide formal lower and upper bounds on the theoretical optimal AUC (AUC^*), characterizing the physical limit of achievable discrimination. The proposed framework applies broadly to interval-valued prediction models, regardless of the interval construction method. Experiments on real-world benchmark datasets, using bootstrap-based intervals as one instantiation, validate the framework’s correctness and demonstrate its practical utility for uncertainty-aware evaluation and decision-making.

1 Introduction

In many high-stakes risk prediction tasks, predicting a single event probability is insufficient, because it does not acknowledge the model’s confidence or lack thereof regarding the true event or label probability. A prediction accompanied by a measure of uncertainty enables more careful decision-making: confident predictions may be acted upon immediately, whereas uncertain cases can be deferred to human review. This is particularly important in medical risk prediction, where model outputs are often used to guide screening, diagnosis, or treatment decisions. For example, in diabetes risk screening, an uncertainty-aware model might output a predicted risk of 0.45 with a 95% confidence interval of [0.25, 0.65]. If this interval lies entirely above a clinical decision threshold, immediate intervention may be justified, whereas if it spans the threshold, further testing or specialist consultation may be warranted.

Motivated by this need, modern uncertainty quantification methods often produce *interval-valued predictions* rather than point estimates. Examples include prediction intervals derived from Bayesian credible intervals, bootstrap procedures, and ensemble methods [Efron and Tibshirani, 1994, Gelman et al., 2013, Gal and Ghahramani, 2016]. For each input X , the model outputs an interval $(L(X), U(X))$ that intends to contain the true event or label probability. While these methods provide richer predictive information, they raise more questions: how can we enhance our

evaluation of uncertainty-aware classification beyond point-based metrics, and how can the quality of our prediction intervals be evaluated when the true event probabilities are unobserved?

Standard evaluation tools for binary classification were designed for point predictions. The Receiver Operating Characteristic (ROC) curve and its summary statistic, the Area Under the Curve (AUC), remain the most widely used metrics. The classical AUC admits a clear probabilistic interpretation as the probability that a randomly chosen positive instance is ranked above a randomly chosen negative one [Hanley and McNeil, 1982]. This interpretation relies on the ability to rank all instances using a scalar score. While existing methods handle tied scores by assigning partial credit to unranked pairs [Hand and Till, 2001], they are insufficient for interval-valued predictions. In this setting, interval overlap represents explicit ranking ambiguity rather than a mere statistical coincidence of identical scores. Therefore, the induced partial ordering calls for an evaluation framework that directly reflects uncertainty in interval-valued scores.

In current practice, interval predictions are often collapsed to point estimates, such as the mean or midpoint, and then evaluated using the standard AUC [Lakshminarayanan et al., 2017, Kuleshov et al., 2018]. This approach discards uncertainty information and prevents analysis of how interval width or overlap relates to discrimination performance. Alternatively, interval predictions are evaluated through properties such as calibration or coverage, typically reported separately from discrimination metrics [Gneiting and Raftery, 2007, Bracher et al., 2021]. Moreover, in binary prediction settings, coverage of event probabilities is not directly observable and can usually be assessed only through simulation or modeling assumptions. Taken together, these practices treat discrimination and uncertainty as separate concerns, leaving no unified metric for evaluating uncertainty-aware classifiers.

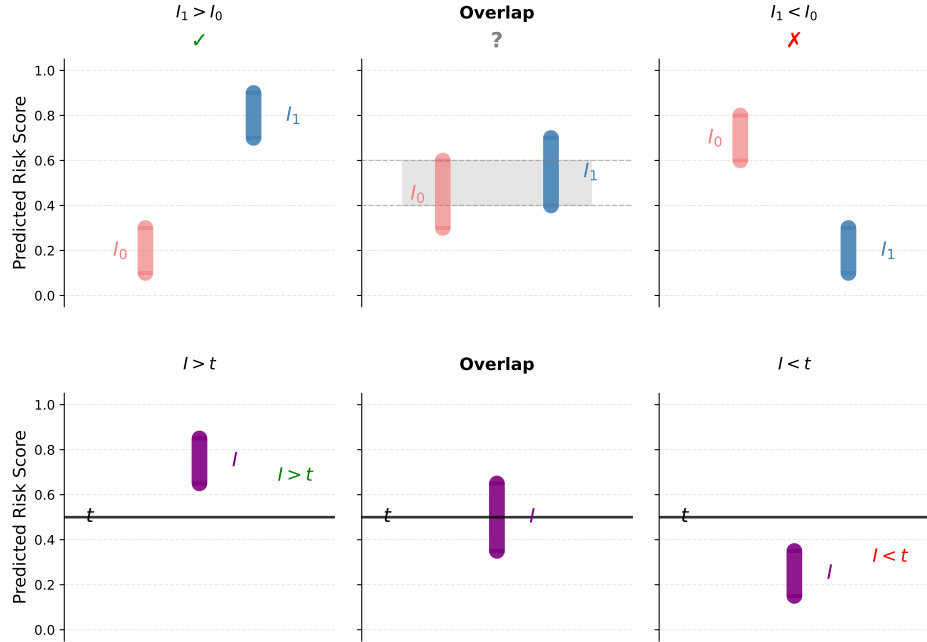


Figure 1: Illustration of interval-based comparisons. **Top:** pairwise comparisons between a positive instance I_1 and a negative instance I_0 . **Bottom:** comparisons between an interval prediction I and a decision threshold t , illustrating confident decisions ($I > t$ or $I < t$) and ambiguity when the interval overlaps the threshold.

In this paper, we develop a rigorous framework for ROC analysis with interval-valued predic-

tions. For two intervals $I_1 = (L_1, U_1)$ and $I_0 = (L_0, U_0)$ from positive and negative classes, we define three comparison outcomes (Figure 1): (i) **confidently correct** if $L_1 > U_0$, (ii) **confidently incorrect** if $U_1 < L_0$, and (iii) **uncertain** if intervals overlap, meaning neither $L_1 > U_0$ nor $U_1 < L_0$ holds. Based on these comparisons, we define two ROC-style curves using rate functions with different levels of strictness: TPR_L vs FPR_U (strict criteria requiring entire intervals to exceed the threshold) and TPR_U vs FPR_L (relaxed criteria allowing intervals to contain the threshold). The areas under these curves are denoted AUC_L and AUC_U , with simple probabilistic interpretations:

$$\text{AUC}_L = \mathbb{P}(I_1 > I_0), \quad \text{AUC}_U = 1 - \mathbb{P}(I_0 > I_1).$$

We first prove that AUC_L and AUC_U equal the probabilities of strict interval orderings (Theorems 1 and 2). Together with the overlap probability, these yield a *three-region decomposition*:

$$\mathbb{P}(I_1 > I_0) + \mathbb{P}(I_1 < I_0) + \mathbb{P}(\text{overlap}) = 1,$$

providing a complete characterization of ranking uncertainty. This decomposition can be visualized geometrically in the ROC plane (Figure 2), where the three probabilities correspond to disjoint regions summing to unity. Unlike the classical AUC, which provides a single scalar value, our framework quantifies the degree to which model-based ranking performance is definitive versus ambiguous.

We further relate interval-based discrimination to the theoretically best achievable ranking performance. The *optimal AUC*, denoted AUC^* , is defined as the supremum of $\mathbb{P}(f(X_1) > f(X_0))$ over all scoring functions f , we show that interval-based discrimination metrics provide informative bounds on AUC^* under mild coverage assumptions. These results connect observable interval predictions to fundamental limits on ranking performance, and clarify how predictive uncertainty constrains achievable discrimination.

We validate the framework empirically using the Pima Indians Diabetes dataset with bootstrap-based prediction intervals. Experiments verify the theoretical equivalences and characterize how interval width affects the three-region decomposition. Our main contributions are: (i) extending ROC analysis to interval-valued predictions with AUC_L and AUC_U metrics; (ii) proving a three-region decomposition of the ROC plane characterizing ranking uncertainty; (iii) establishing bounds on optimal AUC under class-conditional coverage; and (iv) providing practical tools for evaluating selective prediction and uncertainty-aware model selection. This framework offers a principled approach to discrimination analysis for interval-valued predictions.

2 Related Work

Classical ROC Analysis and AUC. The Receiver Operating Characteristic (ROC) curve originated in signal detection theory and is now a standard tool for evaluating binary classifiers Hanley and McNeil [1982], Fawcett [2006]. It plots the true positive rate against the false positive rate as a classification threshold varies, while the area under the curve (AUC) summarizes discriminative ability in a single scalar. A key theoretical result establishes the probabilistic interpretation of AUC: for a scoring function f ,

$$\text{AUC}(f) = \mathbb{P}(f(X^+) > f(X^-)) + \frac{1}{2}\mathbb{P}(f(X^+) = f(X^-)),$$

where X^+ and X^- are independently drawn positive and negative instances. This interpretation links the AUC to pairwise ranking accuracy and underlies its widespread use in applications such as medical risk prediction Pepe [2003]. Numerous extensions have been proposed, including the

partial AUC, cost-sensitive ROC analysis, and multi-class generalizations Fawcett [2006]. Related work has also studied the Bayes-optimal scoring rule that maximizes the AUC under the true data-generating process, often referred to as the optimal AUC Cortes and Mohri [2004], Cléménçon et al. [2008].

Methods Producing Interval-Valued Predictions. A variety of approaches produce interval-valued predictions for binary risk prediction tasks. Bootstrap methods generate empirical prediction distributions by resampling the training data and constructing percentile-based confidence intervals Efron and Tibshirani [1994], DiCiccio and Efron [1996]. Bayesian methods provide posterior predictive distributions from which credible intervals can be derived, including Bayesian generalized linear models, Gaussian processes, and Bayesian neural networks MacKay [1992], Gelman et al. [2013], Gal and Ghahramani [2016]. Ensemble methods estimate uncertainty through variability across models or repeated forward passes, yielding intervals via empirical quantiles Lakshminarayanan et al. [2017]. Our framework is agnostic to the interval generation mechanism and applies to any method that outputs interval-valued predictions.

Evaluation of Prediction Intervals. Standard evaluation metrics for prediction intervals focus on *calibration* and *sharpness*, often following the principle of maximizing sharpness (measured by average width) subject to valid calibration [Gneiting and Raftery, 2007]. These properties are typically assessed via proper scoring rules like the *Weighted Interval Score (WIS)*, or by examining under- and over-coverage rates separately [Bracher et al., 2021]. However, these metrics are fundamentally local and pointwise; they evaluate uncertainty quantification for individual instances but do not characterize the global discriminative performance or ranking consistency [Gneiting and Raftery, 2007]. Furthermore, while group-level calibration is estimable using binary labels, individual-level coverage of the true posterior $\eta(x)$ remains unobservable in real-world settings. Our framework bridges this gap by mapping unobservable coverage properties to observable bounds on the optimal AUC Cléménçon et al. [2008]. This allows practitioners to translate uncertainty guarantees from methods like conformal prediction [Vovk et al., 2005, Angelopoulos and Bates, 2021] into a tangible range of discriminative performance.

Selective Prediction and Abstention. Selective prediction studies decision-making under uncertainty by allowing models to abstain when confidence is low, which enables a trade-off between retention rate and accuracy on the non-abstaining instances [El-Yaniv et al., 2010, Geifman and El-Yaniv, 2019]. Conventional approaches typically rely on scalar confidence scores to implement pointwise rejection, with most research focusing on label prediction and the empirical estimation of thresholds to control error rates. However, this literature primarily focuses on decision policies for individual labels rather than on how uncertainty propagates to ranking or global discrimination metrics [El-Yaniv et al., 2010]. Furthermore, while label-based confidence can be verified directly against observed outcomes, there is no inherent way to assess the coverage of second-order uncertainty quantification, which captures uncertainty over the predicted probabilities themselves, as the true posterior $\eta(x)$ remains unobservable in real-world binary data. Our framework addresses this gap by characterizing how interval-valued predictions induce pairwise ranking ambiguity. Instead of rejecting individual points, we utilize interval overlaps to identify ambiguous pairs and assess discrimination via the **uncertainty-aware AUC** (see Section 3.4), which measures the fraction of non-overlapping pairs that are correctly ordered.

Research Gap and Our Contribution. Taken together, existing work provides well-developed tools for evaluating scalar classifiers and for assessing the calibration and sharpness of prediction intervals. What remains missing is a principled framework to incorporate interval-valued uncertainty into discrimination analysis. In particular, existing metrics do not quantify ranking ambiguity induced by overlapping intervals, nor do they provide AUC-style summaries that account for uncertainty. This paper fills this gap by extending ROC analysis to interval-valued predictions, providing probabilistic interpretations, and introducing the *uAUC* metric for uncertainty-aware evaluation. Furthermore, by linking uncertainty calibration directly to bounds on the optimal AUC under class-conditional coverage, our framework enables practitioners to translate observable interval predictions into a tangible range of the best achievable discrimination.

3 Setup and Theory

3.1 Problem Setup and Interval Comparisons

We consider a binary risk prediction problem with labels $Y \in \{0, 1\}$, where $Y = 1$ denotes the positive class and $Y = 0$ the negative class. The goal is to predict a continuous risk score associated with the positive class, which can subsequently be used to support threshold-based decisions. Instead of scalar prediction scores, we suppose the classifier outputs an interval-valued score $I(x) = (L(x), U(x))$, where $L(x) \leq U(x)$ for each input x .

Let $I_1 = (L_1, U_1)$ and $I_0 = (L_0, U_0)$ denote random prediction intervals obtained by applying this scoring rule to independent draws from the positive and negative class distributions, respectively. Note that we use subscripts 1 and 0 to denote conditioning on the true class label, and this pairwise notation is used to characterize ranking behavior. We write $I_1 \sim F_1$ and $I_0 \sim F_0$ for the corresponding distributions over intervals. Throughout, we assume $L_i \leq U_i$ almost surely for $i \in \{0, 1\}$.

We compare interval-valued scores using strict non-overlap criteria, under which one object is ranked above another only when the ordering is unambiguous given the reported uncertainty. For an interval $I = (L, U)$ and a threshold $t \in \mathbb{R}$, we write $I > t$ if $L > t$ and $I < t$ if $U < t$, requiring the entire interval to lie on one side of the threshold. Similarly, for two intervals $I_1 = (L_1, U_1)$ and $I_0 = (L_0, U_0)$, we define

$$I_1 > I_0 \iff L_1 > U_0, \quad I_1 < I_0 \iff U_1 < L_0.$$

If neither condition holds, the intervals overlap. Figure 1 illustrates the three cases. These rules induce a partial ordering that distinguishes definitively ordered pairs from ambiguous ones.

3.2 Two ROC-Style Curves and Interval-Based AUC Quantities

Using interval-threshold comparisons, we define four rate functions, where TPR and FPR denote the true positive rate and false positive rate, respectively, for a threshold $t \in \mathbb{R}$:

$$\begin{aligned} \text{TPR}_L(t) &= \mathbb{P}(L_1 > t), & \text{TPR}_U(t) &= \mathbb{P}(U_1 > t), \\ \text{FPR}_L(t) &= \mathbb{P}(L_0 > t), & \text{FPR}_U(t) &= \mathbb{P}(U_0 > t). \end{aligned}$$

By construction, $\text{TPR}_L(t) \leq \text{TPR}_U(t)$ and $\text{FPR}_L(t) \leq \text{FPR}_U(t)$ for all t .

We define two ROC-style curves by pairing rate functions with different levels of strictness. The first curve plots $\text{TPR}_L(t)$ against $\text{FPR}_U(t)$ as t varies, and the second plots $\text{FPR}_L(t)$ against

$\text{TPR}_U(t)$. The associated areas under these curves are denoted by

$$\text{AUC}_L = \int \text{TPR}_L(t) d[\text{FPR}_U(t)], \quad (1)$$

$$\text{AUC}_U = \int \text{TPR}_U(t) d[\text{FPR}_L(t)]. \quad (2)$$

The pairing of rate functions reflects different notions of conservativeness in interval-based discrimination. The curve $(\text{TPR}_L, \text{FPR}_U)$ corresponds to a strict comparison rule. Here, TPR_L is conservative in that a positive instance contributes to the true positive rate only if its entire interval lies above the threshold, while FPR_U is conservative in the opposite direction, counting a negative instance as a false positive whenever any part of its interval exceeds the threshold. Together, this pairing yields a conservative assessment of discrimination that requires certainty for correct rankings and penalizes any potential error.

In contrast, the curve $(\text{TPR}_U, \text{FPR}_L)$ corresponds to a permissive rule. Under this pairing, TPR_U credits a positive instance whenever the threshold is at least partially exceeded, while FPR_L penalizes a negative instance only when its entire interval exceeds the threshold. This rule favors potential separation and yields an upper bound on discriminative performance under interval uncertainty.

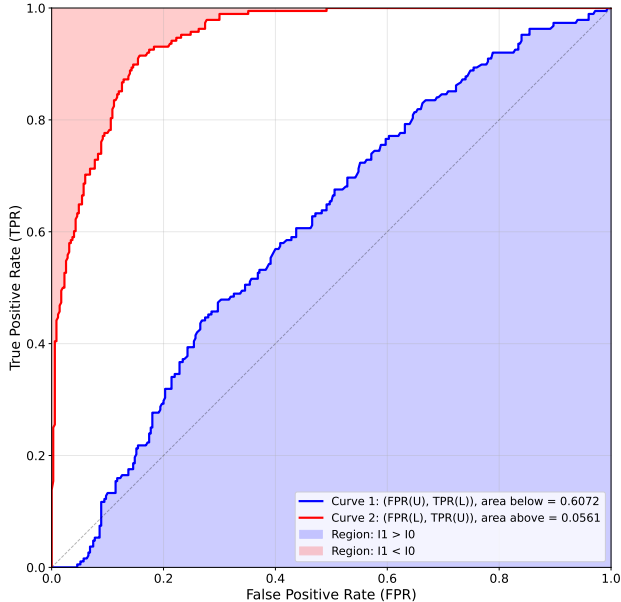


Figure 2: Geometric interpretation of interval-based ROC analysis. The blue curve plots TPR_L versus FPR_U (area = AUC_L), and the red curve plots TPR_U versus FPR_L (area above = $1 - \text{AUC}_U$). The three regions correspond to $\mathbb{P}(I_1 > I_0)$ (blue), $\mathbb{P}(\text{overlap})$ (white), and $\mathbb{P}(I_1 < I_0)$ (red). Curves are shown for a 90% confidence level from Experiment 1 in Section 5.2.

3.3 Main Theoretical Results

A key property of the classical AUC is its probabilistic interpretation as $\text{AUC} = \mathbb{P}(f(X_1) > f(X_0))$, the probability that a randomly chosen positive instance is ranked above a randomly chosen negative one. We show that this property extends naturally to interval-valued predictions, yielding analogous interpretations for AUC_L and AUC_U .

For a randomly chosen positive interval $I_1 = (L_1, U_1)$ and an independently chosen negative interval $I_0 = (L_0, U_0)$, the following two results hold:

Theorem 1.

$$\text{AUC}_L = \mathbb{P}(L_1 > U_0) = \mathbb{P}(I_1 > I_0). \quad (3)$$

Proof. Let $G_1(l) = \mathbb{P}(L_1 \leq l)$ and $H_0(u) = \mathbb{P}(U_0 \leq u)$. Since $\text{TPR}_L(t) = \mathbb{P}(L_1 > t) = 1 - G_1(t)$ and $\text{FPR}_U(t) = \mathbb{P}(U_0 > t) = 1 - H_0(t)$, we have $d[\text{FPR}_U(t)] = -dH_0(t)$. Therefore,

$$\begin{aligned} \text{AUC}_L &= \int (1 - G_1(t)) d(1 - H_0(t)) \\ &= \mathbb{E}_{U_0}[1 - G_1(U_0)] \\ &= \mathbb{P}(L_1 > U_0), \end{aligned}$$

□

Theorem 2.

$$\text{AUC}_U = 1 - \mathbb{P}(U_1 < L_0) = 1 - \mathbb{P}(I_1 < I_0). \quad (4)$$

Proof. This follows by an analogous argument, exchanging the roles of (L_1, U_1) and (L_0, U_0) in the preceding proof. □

Corollary 1 (Three-Region Decomposition).

$$\mathbb{P}(I_1 > I_0) + \mathbb{P}(I_1 < I_0) + \mathbb{P}(\text{overlap}) = 1, \quad (5)$$

where *overlap* is defined by $L_1 \leq U_0$ and $U_1 \geq L_0$.

Geometric Interpretation Plotting the two ROC-style curves in the unit square yields a natural geometric interpretation of interval-based discrimination (Figure 2). The area below the TPR_L – FPR_U curve equals $\mathbb{P}(I_1 > I_0)$, while the area above the reflected TPR_U – FPR_L curve corresponds to $\mathbb{P}(I_1 < I_0)$. The remaining region represents the probability of overlap, capturing ranking ambiguity induced by interval-valued predictions.

Connection to Classical AUC When prediction intervals collapse to points, that is, $L = U$ almost surely, the overlap probability vanishes and the partial ordering becomes total. In this case, $\text{TPR}_L(t) = \text{TPR}_U(t)$, and $\text{FPR}_L(t) = \text{FPR}_U(t)$, so that $\text{AUC}_L = \text{AUC}_U$ reduces to the classical AUC. Thus, the proposed framework recovers standard ROC analysis as a special case.

3.4 Selective Prediction and Uncertainty-Aware AUC

Beyond pure evaluation, the proposed framework naturally supports *selective prediction* by identifying pairs where the model should abstain due to ranking ambiguity. In this context, the classifier provides a definitive ordering for a pair (X_1, X_0) only if their prediction intervals do not overlap.

To quantify the discriminative performance on these decisive cases, we define the **uncertainty-aware AUC** (*uAUC*) as the conditional probability of a correct ranking given that a decisive ordering exists:

$$u\text{AUC} := \frac{\mathbb{P}(I_1 > I_0)}{\mathbb{P}(I_1 > I_0) + \mathbb{P}(I_1 < I_0)}. \quad (6)$$

The *uAUC* captures the intrinsic quality of the model's high-confidence rankings. A fundamental property of this metric is that its reliability should not degrade—and typically improves—as the uncertainty requirements become more stringent. This is formalized in the following proposition.

Proposition 1 (Monotonicity of $uAUC$). *Let $I(x, \gamma)$ be a symmetric prediction interval centered at a score $s(x)$, with half-width $\delta(x, \gamma)$ that is non-decreasing in the confidence level $\gamma \in (0, 1)$. Assume that the probability of a correct ranking, $\mathbb{P}(s(X_1) > s(X_0)$ is correct $| |s(X_1) - s(X_0)| = \Delta s$, is a non-decreasing function of the score difference Δs . Then the uncertainty-aware AUC, $uAUC(\gamma)$, is non-decreasing in γ .*

This result guarantees that the interval-based framework acts as a valid filter for ranking reliability: as the confidence level γ increases, the model abstains more frequently but maintains or improves the quality of its definitive decisions. The proof is provided in Appendix A.

4 Estimating the Bounds of the Optimal AUC

In this section, we investigate the relationship between our proposed interval-based metrics and the theoretical limit of discriminative performance. We show that under mild coverage assumptions, AUC_L and AUC_U provide principled bounds on the optimal AUC achievable by any scoring function.

4.1 Optimal AUC and Bayes-Optimal Ranking

Let $(X, Y) \sim P$ with labels $Y \in \{0, 1\}$. We define the true (unknown) posterior probability (the regression function) as $\eta(x) = \mathbb{P}(Y = 1 | X = x)$. For any measurable scoring function $f : \mathcal{X} \rightarrow \mathbb{R}$, its population-level AUC is defined as $AUC(f) = \mathbb{P}(f(X_1) > f(X_0))$, where $X_1 \sim P(X | Y = 1)$ and $X_0 \sim P(X | Y = 0)$ are independent. The *optimal AUC*, denoted by AUC^* , is the maximum ranking performance attainable under the true data distribution:

$$AUC^* := \sup_f AUC(f). \quad (7)$$

A fundamental result in statistical learning theory shows that the Bayes posterior $\eta(x)$ induces the optimal ranking. As shown by Clémenton et al. [2008], any scoring function that is a strictly monotone transformation of $\eta(x)$ maximizes the ROC curve at every point and thus achieves AUC^* :

$$AUC^* = \mathbb{P}(\eta(X_1) > \eta(X_0)). \quad (8)$$

This value represents the physical limit of discrimination due to the intrinsic overlap of class-conditional distributions.

4.2 Bounding Optimal AUC under Marginal Coverage

While $\eta(x)$ is generally unknown, interval-valued predictions $I(x) = [L(x), U(x)]$ allow us to reason about the location of $\eta(x)$ with a certain degree of confidence. To link $I(x)$ to AUC^* , we assume the intervals satisfy class-conditional coverage guarantees. Let the miscoverage rates be defined as:

$$\alpha_i := \mathbb{P}(\eta(X) \notin I(X) | Y = i), \quad i \in \{0, 1\}. \quad (9)$$

For a randomly drawn pair (X_1, X_0) , we define the *pairwise coverage event* E_{pair} as the case where both intervals correctly capture their respective posterior probabilities:

$$E_{\text{pair}} := \{\eta(X_1) \in I(X_1)\} \cap \{\eta(X_0) \in I(X_0)\}. \quad (10)$$

Assuming independence between X_1 and X_0 , the probability that at least one interval fails to cover η , denoted as p_{pair} , is:

$$p_{\text{pair}} := \mathbb{P}(E_{\text{pair}}^c) = 1 - (1 - \alpha_1)(1 - \alpha_0) = \alpha_1 + \alpha_0 - \alpha_1\alpha_0. \quad (11)$$

In practice, when α_1, α_0 are small, p_{pair} can be tightly approximated by $\alpha_1 + \alpha_0$.

On the event E_{pair} , the strict interval ordering directly implies the Bayes ordering. Specifically, if $L_1 > U_0$, then $\eta(X_1) \geq L_1 > U_0 \geq \eta(X_0)$, which necessitates $\eta(X_1) > \eta(X_0)$. Conversely, if $\eta(X_1) > \eta(X_0)$, it must hold that $U_1 > L_0$ for any overlapping or correctly ordered intervals. This logical connection allows us to bound the optimal AUC using observable interval-based quantities.

Theorem 3 (Bounds on the Optimal AUC). *Given interval-valued predictions $I(x)$ with class-conditional miscoverage rates α_1 and α_0 , the optimal AUC satisfies:*

$$\text{AUC}_L - p_{\text{pair}} \leq \text{AUC}^* \leq \text{AUC}_U + p_{\text{pair}}. \quad (12)$$

The proof is provided in Appendix B.

This result provides a principled way to estimate the range of the best achievable discrimination. As the model's uncertainty quantification becomes more precise (shorter intervals) while maintaining coverage (small α), AUC_L and AUC_U converge toward each other, effectively sandwiching the optimal AUC. This framework allows practitioners to quantify not just how well their current model performs, but also how much room remains for improvement relative to the Bayes-optimal limit.

5 Experiments

We illustrate and empirically validate the proposed interval-based AUC framework on the Pima Indians Diabetes dataset. Our evaluation focuses on verifying the theoretical equivalences and characterizing the dynamics of ranking ambiguity. In addition, we demonstrate how the proposed framework supports selective prediction by abstaining on uncertain cases and examining the trade-off between the abstention rate and uncertainty-aware ranking performance as measured by AUC_L and AUC_U .

5.1 Experimental Setup

The Pima dataset contains clinical measurements from 768 female patients aged 21 and above, with 8 features. The binary outcome indicates diabetes onset within five years. The dataset is partitioned into a 30% training (230 samples) and 70% test (538 samples) split with stratification to preserve the class distribution.

We train a logistic regression classifier with standard feature scaling using bootstrap resampling. For each test instance x_i , we fit 300 logistic regression models on bootstrap samples of the training data and obtain predicted probabilities. Prediction intervals at level $(1 - \alpha)$ are constructed using empirical quantiles of the bootstrap predictions, with lower and upper bounds given by $L_i = Q_{\alpha/2}$ and $U_i = Q_{1-\alpha/2}$, yielding interval-valued predictions $I(x_i) = [L_i, U_i]$. As a reference, the baseline point AUC computed from mean predicted probabilities is 0.831.

5.2 Empirical Results and Analysis

Experiment 1: Validation of AUC-Probability Equivalence. We first verify the core theoretical results of Theorems 1 and 2 on real data. Using 90% confidence intervals, we compute

AUC_L via trapezoidal integration of the TPR_L vs FPR_U curve and compare it with the empirical estimate $\mathbb{P}(I_1 > I_0)$ obtained by counting pairwise interval comparisons. Similarly, we compute AUC_U from the FPR_L vs TPR_U curve and verify its relationship with $1 - \mathbb{P}(I_1 < I_0)$.

Table 1: Empirical validation of AUC–probability equivalence at 90% CI. All discrepancies are below 0.02%.

Quantity	Value	Diff
AUC_L vs. $\mathbb{P}(I_1 > I_0)$	0.6074 / 0.6072	0.0002
AUC_U vs. $1 - \mathbb{P}(I_1 < I_0)$	0.9427 / 0.9439	0.0013
$\mathbb{P}(I_1 > I_0)$	0.6072	—
$\mathbb{P}(\text{overlap})$	0.3367	—
$\mathbb{P}(I_1 < I_0)$	0.0561	—
Sum of probabilities	1.0000	—

Table 1 summarizes the results. The difference between AUC_L and $\mathbb{P}(I_1 > I_0)$ is less than 0.02%, and a similarly small discrepancy is observed for AUC_U , confirming the theoretical equivalences. The three probabilities sum to 1.0000, validating Corollary 1. With 90% confidence intervals, we observe $\mathbb{P}(I_1 > I_0) = 0.607$, indicating that approximately 61% of pairwise rankings are definitively correct, $\mathbb{P}(\text{overlap}) = 0.337$ are uncertain, and $\mathbb{P}(I_1 < I_0) = 0.056$ are confidently incorrect. By contrast, a standard AUC-based evaluation would collapse these outcomes into a single estimate, reporting that approximately 83.1% of pairwise rankings are correct and 16.9% are incorrect. This aggregation obscures the fact that only a small fraction of errors are made with high confidence, while a substantial portion of comparisons are fundamentally ambiguous due to interval overlap. Figure 2 visualizes the combined ROC-style curves in the unit square, showing the three-region decomposition geometrically.

Experiment 2: Three-Region View of Interval-Induced Discrimination. We examine how interval width affects discrimination by varying the confidence level from 50% to 95% (Table 2). Narrow intervals (50% CI) yield well-separated predictions with low overlap, while wide intervals (95% CI) produce substantial ambiguity.

At 50% confidence, the interval-based metrics indicate strong discrimination, with $\text{AUC}_L = 0.749$ and $\mathbb{P}(\text{overlap}) = 0.142$. As the confidence level increases, AUC_L decreases while $\mathbb{P}(\text{overlap})$ increases, reaching 0.559 and 0.398 at 95% confidence, respectively. At the same time, AUC_U increases as the interval constraints become less restrictive. Together, these metrics summarize how increasing interval width degrades discrimination by reducing the fraction of decisively ordered pairs.

Table 2: Effect of confidence level on interval-based metrics. Narrower intervals (50% CI) reduce overlap but may undercover; wider intervals (95% CI) increase overlap but ensure higher coverage.

CI Level	AUC_L	AUC_U	$\mathbb{P}(\text{overlap})$
50%	0.7492	0.8914	0.1423
70%	0.6997	0.9139	0.2142
90%	0.6072	0.9439	0.3367
95%	0.5585	0.9562	0.3977

The three-region decomposition, $\mathbb{P}(I_1 > I_0) + \mathbb{P}(\text{overlap}) + \mathbb{P}(I_1 < I_0) = 1$, provides a structural interpretation of this redistribution. Figure 3 visualizes the evolution of these regions across confidence levels. At 0% CI, the overlap region is absent and $\mathbb{P}(I_1 > I_0)$ recovers the classical point-based AUC. As intervals widen, probability mass shifts primarily from $\mathbb{P}(I_1 > I_0)$ to the overlap region, while the rate of confident misorderings $\mathbb{P}(I_1 < I_0)$ remains uniformly low (< 10%). This indicates that wider intervals favor caution, converting previously decisive comparisons into ambiguous ones rather than inducing high-confidence ranking reversals. Consequently, the scalar trends in Table 2 reflect projections of this global redistribution onto summary measures such as AUC_L and AUC_U .

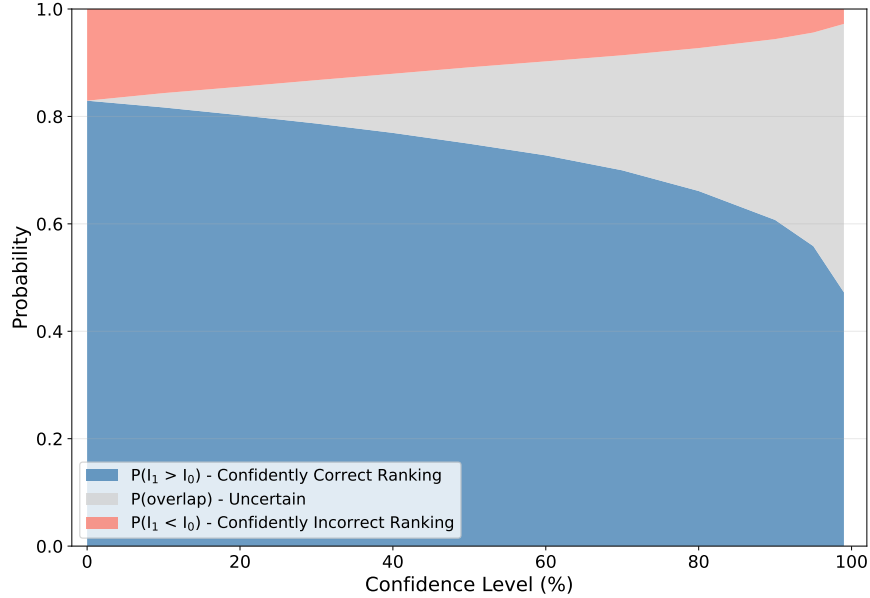


Figure 3: Three-region Decomposition vs. Confidence level. The stacked areas show $\mathbb{P}(I_1 > I_0)$ (blue, confidently correct rankings), $\mathbb{P}(\text{overlap})$ (gray, ambiguous rankings), and $\mathbb{P}(I_1 < I_0)$ (red, confidently incorrect rankings). At 0% confidence level, the decomposition reduces to the classical point-based case with no overlap. As the confidence level increases from 0% to 99%, probability mass shifts from ordered regions to the overlap region, while the total probability remains equal to 1.

Experiment 3: Selective Prediction Our framework naturally supports selective prediction by identifying pairs where the model should *abstain* due to ranking ambiguity. The **uncertainty-aware AUC** ($u\text{AUC}$) is defined as the conditional probability of a correct ordering given that the intervals do not overlap (see equation (6)). Physically, $u\text{AUC}$ quantifies the discriminative quality of the model’s *definitive* decisions. At a 90% confidence level, the classifier abstains on 33.7% of pairs (AR = 0.337) but achieves a $u\text{AUC}$ of 0.916 on the remaining instances, significantly exceeding the baseline point-AUC of 0.8306.

As shown in Figure 4, as the confidence level increases from 50% to 99%, the abstention rate rises while the $u\text{AUC}$ steadily increases. This stability is a crucial finding: it suggests that the interval-based framework effectively filters out inherently ambiguous pairs while preserving a highly reliable discriminative core. For safety-critical tasks like medical screening, this allows practitioners to set an abstention threshold that guarantees a target level of ranking reliability.

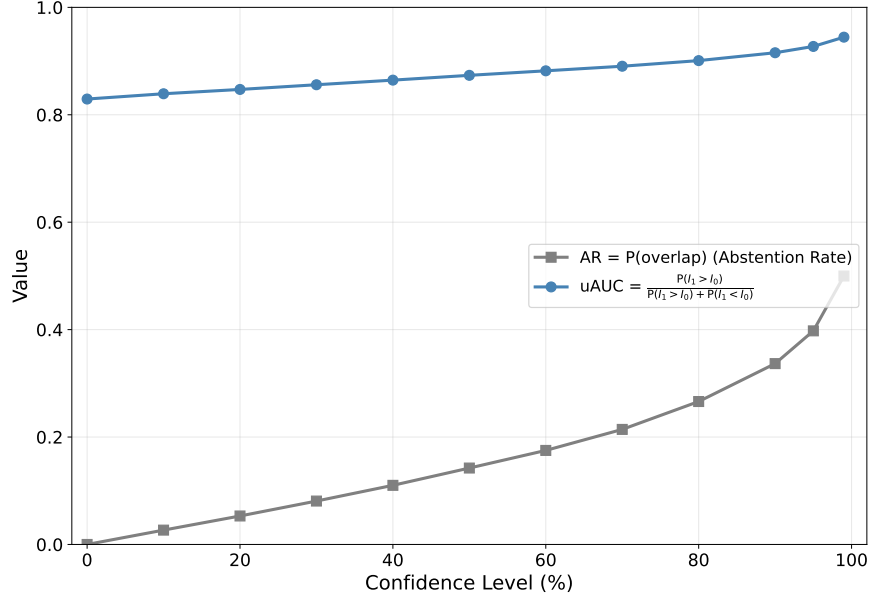


Figure 4: Selective prediction metrics versus nominal confidence level. The abstention rate (AR, gray) increases with interval width, while the uncertainty-aware AUC ($uAUC$, blue) remains stable (0.83–0.94) and monotonically increasing.

5.3 Empirical Validation of Optimal AUC Bounds

We empirically validate Theorem 3 using a synthetic experiment in which the true posterior $\eta(x)$ is known, allowing for the direct calculation of the Bayes-optimal AUC.

Experimental Setup. We consider a binary classification task with a 1D feature X following $P(X|Y = i) = \mathcal{N}(\mu_i, 1)$. To focus on the high-ambiguity regime where uncertainty-aware evaluation is most critical, we set $\mu_0 = 0$ and $\mu_1 = 1$ as a stress test, yielding a ground-truth $AUC^* = 0.764$. For a given miscoverage rate α , we construct prediction intervals $I(x) = [L(x), U(x)]$ with half-width $\delta = 0.05 + 0.3\alpha + 0.1 \text{std}(\eta)$. Intervals are centered at $\eta(x)$ for a $(1 - \alpha)$ fraction of samples, while miscoverage is induced for the remaining α fraction by shifting centers by $\delta + \epsilon$, where $\epsilon \sim \text{Uniform}(0.01, 0.1)$. All interval boundaries are clipped to $[0, 1]$.

Results. As shown in Figure 5, the optimal AUC^* is strictly contained within the theoretical bounds across all evaluated miscoverage rates. As α increases, the bounds widen monotonically, reflecting the explicit dependence on the pairwise miscoverage probability p_{pair} . At $\alpha = 0.01$, the bound width is 0.328, corresponding to the interval $[0.574, 0.903]$. At $\alpha = 0.05$, the bound expands to $[0.459, 0.992]$. This behavior is expected in a high-overlap setting, where a large fraction of pairwise comparisons is inherently ambiguous and cannot be resolved without stronger assumptions.

The width of these bounds reflects the conservatism inherent to distribution-free guarantees in high-overlap settings. Rather than providing a tight performance estimate, the bounds characterize the range of Bayes-optimal discrimination compatible with the observed interval uncertainty. In this regime, the gap between AUC_L and AUC_U serves as a quantitative indicator of ranking ambiguity, reflecting the information limitations imposed by substantial feature overlap.

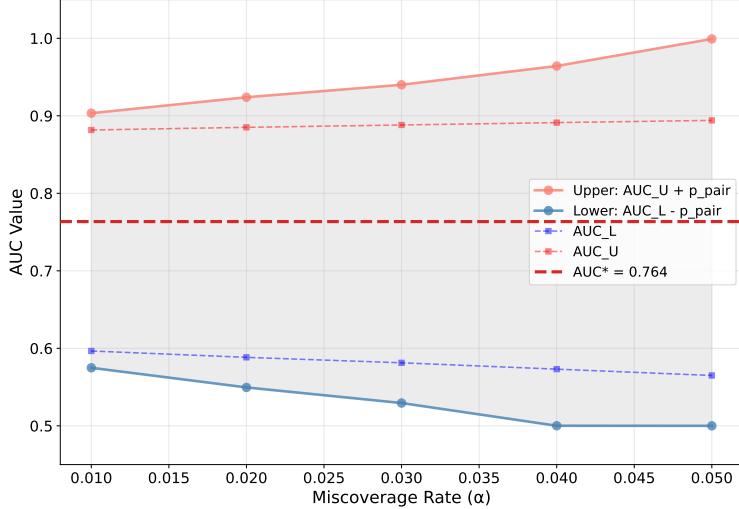


Figure 5: Empirical validation of theoretical bounds on the optimal AUC (AUC^*). The shaded region denotes the theoretical range $[AUC_L - p_{\text{pair}}, AUC_U + p_{\text{pair}}]$, which strictly contains the optimal AUC across varying miscoverage rates α .

5.4 Summary

The empirical results on real-world medical data validate the theoretical properties of AUC_L , AUC_U , and the three-region decomposition with high precision. By identifying ranking ambiguity, our framework supports selective prediction strategies that yield significant benefits in high-stakes risk prediction tasks. Furthermore, we establish conservative bounds on the optimal AUC, providing a principled range for the best achievable discrimination under observed interval uncertainty.

6 Discussion and Conclusion

This paper introduces the iAUC framework, extending ROC analysis to accommodate interval-valued predictions. By defining AUC_L and AUC_U , we provide a principled way to evaluate uncertainty-aware classifiers beyond point-score metrics that discard confidence information. The core of our framework is the three-region decomposition, which partitions pairwise rankings into correct, incorrect, and ambiguous categories. Experiments demonstrate that this decomposition reveals how predictive uncertainty converts decisive rankings into overlaps rather than high-confidence errors, clarifying model reliability in high-stakes tasks.

Furthermore, we established a formal link between interval-based metrics and theoretical discrimination limits. Under valid coverage, AUC_L and AUC_U provide informative bounds on the optimal AUC. The $uAUC$ metric further enables selective prediction by abstaining on ambiguous pairs while maintaining a highly reliable discriminative core. Future work may explore multi-class settings or integration with conformal prediction for tighter guarantees. In conclusion, iAUC offers a rigorous, practical toolkit for evaluating and deploying uncertainty-aware classification models.

References

Anastasios N Angelopoulos and Stephen Bates. A gentle introduction to conformal prediction and distribution-free uncertainty quantification. *arXiv preprint arXiv:2107.07511*, 2021. A modern,

popular tutorial for machine learning practitioners.

Johannes Bracher, Evan L Ray, Tilmann Gneiting, and Nicholas G Reich. Evaluating epidemic forecasts in an interval format. *Journal of the American Statistical Association*, 2021.

Stéphan Clémençon, Gábor Lugosi, and Nicolas Vayatis. Ranking and empirical minimization of u-statistics. *The Annals of Statistics*, 36(2):844–874, 2008. doi: 10.1214/009052607000000910.

Corinna Cortes and Mehryar Mohri. Auc optimization vs. error rate minimization. In *Advances in Neural Information Processing Systems*, 2004.

Thomas J DiCiccio and Bradley Efron. Bootstrap confidence intervals. *Statistical Science*, 11(3):189–228, 1996.

Bradley Efron and Robert J Tibshirani. *An Introduction to the Bootstrap*. Chapman and Hall/CRC, 1994.

Ran El-Yaniv et al. On the foundations of noise-free selective classification. *Journal of Machine Learning Research*, 11:1605–1641, 2010.

Tom Fawcett. An introduction to roc analysis. *Pattern Recognition Letters*, 27(8):861–874, 2006.

Yarin Gal and Zoubin Ghahramani. Dropout as a bayesian approximation: Representing model uncertainty in deep learning. In *International Conference on Machine Learning*, 2016.

Yonatan Geifman and Ran El-Yaniv. Selectivenet: A deep neural network with an integrated reject option. In *International Conference on Machine Learning*, 2019.

Andrew Gelman, John B Carlin, Hal S Stern, David B Dunson, Aki Vehtari, and Donald B Rubin. *Bayesian Data Analysis*. CRC Press, 2013.

Tilmann Gneiting and Adrian E Raftery. Strictly proper scoring rules, prediction, and estimation. *Journal of the American Statistical Association*, 102(477):359–378, 2007.

David J. Hand and Robert J. Till. A simple generalisation of the area under the roc curve for multiple class classification problems. *Machine Learning*, 45(2):171–186, 2001.

James A Hanley and Barbara J McNeil. The meaning and use of the area under a receiver operating characteristic (roc) curve. *Radiology*, 143(1):29–36, 1982.

Volodymyr Kuleshov, Nathan Fenner, and Stefano Ermon. Accurate uncertainties for deep learning using calibrated regression. In *International Conference on Machine Learning*, 2018.

Balaji Lakshminarayanan, Alexander Pritzel, and Charles Blundell. Simple and scalable predictive uncertainty estimation using deep ensembles. In *NeurIPS*, 2017.

David JC MacKay. A practical Bayesian framework for backpropagation networks. *Neural Computation*, 4(3):448–472, 1992.

Margaret S Pepe. *The Statistical Evaluation of Medical Tests for Classification and Prediction*. Springer, 2003.

Vladimir Vovk, Alex Gammerman, and Glenn Shafer. *Algorithmic Learning in a Random World*. Springer, 2005.

A Proof of Proposition 1

Proof. For a given confidence level γ , let $\Omega(\gamma) = \delta(X_1, \gamma) + \delta(X_0, \gamma)$ be the combined width threshold. We define the decisive (non-overlapping) event as $A_\gamma := \{|s(X_1) - s(X_0)| > \Omega(\gamma)\}$. By definition, the uncertainty-aware AUC is the conditional expectation:

$$uAUC(\gamma) = \mathbb{E}[\mathbf{1}\{\text{correct ranking}\} \mid A_\gamma]. \quad (13)$$

Since $\delta(x, \gamma)$ is non-decreasing in γ for all x , the threshold $\Omega(\gamma)$ is also non-decreasing. It follows that for any $\gamma_1 < \gamma_2$, the decisive events satisfy the nesting property $A_{\gamma_2} \subseteq A_{\gamma_1}$.

Let $h(\Delta s) = \mathbb{P}(\text{correct ranking} \mid \Delta s)$ be the ranking accuracy function, which is non-decreasing by assumption. The $uAUC(\gamma)$ can be expressed as a truncated expectation of $h(\Delta s)$:

$$uAUC(\gamma) = \mathbb{E}[h(\Delta s) \mid \Delta s > \Omega(\gamma)]. \quad (14)$$

As γ increases, the condition $\Delta s > \Omega(\gamma)$ restricts the expectation to a subset of pairs with strictly larger score differentials. Because $h(\Delta s)$ is non-decreasing, the average accuracy over this more restrictive set must be greater than or equal to that of the broader set. Therefore, $uAUC(\gamma_2) \geq uAUC(\gamma_1)$, which completes the proof. \square

B Proof of Theorem 3

Proof. Let E_{pair} denote the event that both interval predictions cover the corresponding Bayes posterior values, that is,

$$E_{\text{pair}} := \{\eta(X_1) \in I_1\} \cap \{\eta(X_0) \in I_0\},$$

and let $p_{\text{pair}} = \mathbb{P}(E_{\text{pair}}^c)$.

For the lower bound, observe that whenever E_{pair} holds,

$$L_1 > U_0 \Rightarrow \eta(X_1) > \eta(X_0).$$

This implies the pointwise inequality

$$\mathbf{1}\{L_1 > U_0\} \leq \mathbf{1}\{\eta(X_1) > \eta(X_0)\} + \mathbf{1}\{E_{\text{pair}}^c\}.$$

Taking expectations yields

$$\text{AUC}_L \leq \text{AUC}^* + p_{\text{pair}},$$

or equivalently $\text{AUC}_L - p_{\text{pair}} \leq \text{AUC}^*$.

For the upper bound, note that under E_{pair} ,

$$\eta(X_1) > \eta(X_0) \Rightarrow U_1 > L_0.$$

Hence,

$$\mathbf{1}\{\eta(X_1) > \eta(X_0)\} \leq \mathbf{1}\{U_1 > L_0\} + \mathbf{1}\{E_{\text{pair}}^c\}.$$

Taking expectations gives

$$\text{AUC}^* \leq \text{AUC}_U + p_{\text{pair}}.$$

Combining the two bounds completes the proof. \square